THE JOURNAL OF PHYSICAL CHEMISTRY Letters

pubs.acs.org/JPCL Letter

Observing the Fluctuation Dynamics of Dative Bonds Using Two-Dimensional Electronic Spectroscopy

Thanh Nhut Do, Jamie Hung Ni Sim, Hoang Long Nguyen, Yunpeng Lu, and Howe-Siang Tan*

Cite This: *J. Phys. Chem. Lett.* 2021, 12, 165–170 Read Online

ACCESS | Metrics & More | Article Recommendations | Supporting Information

ABSTRACT: We perform two-dimensional electronic spectroscopy on chlorophyll (Chl) *a* and *b* molecules in aprotic solvents of different Lewis basicity. By analyzing the ultrafast spectral diffusion dynamics of the Q_y transition, we show that a certain timescale of the spectral diffusion dynamics is affected by the solvents' Lewis basicity. Control experiments with Chlorin-e6—a Chl molecule analog—and *ab initio* time-dependent density functional theory calculations confirm that we are directly probing the fluctuation dynamics of the dative bond between the solvent's lone pair and the Mg^{2+} center in Chls that is responsible for the Lewis basicity. The observation is indicative of dative bond length and angular fluctuations with timescales ranging between ∼30 and 150 ps and the dative bond-strength-dependent perturbation on the Q_y transition frequency of Chls.

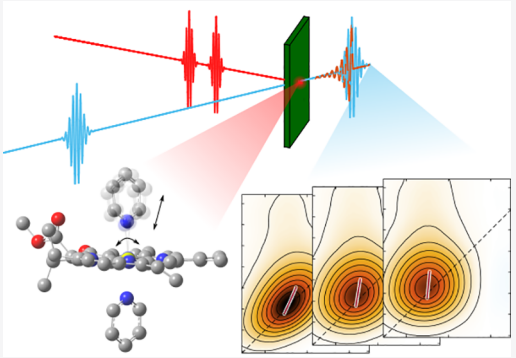

In this study, we provide a time-resolved molecular level study at the ultrafast timescale of a specific molecular process—the fluctuation and bond-breaking/forming process of a dative bond. The dative bond studied is that between the Mg^{2+} center in chlorophyll (Chl) molecules and the lone pair of a solvent, which is associated with the macroscopic chemical property of Lewis basicity. This is achieved by measuring the ultrafast spectral diffusion dynamics of Chl *a* and Chl *b* in various solvents of different Lewis basicity using two-dimensional electronic spectroscopy (2DES).

Chlorophyll is the main pigment responsible for the light-harvesting and energy regulation processes of most photosynthetic organisms on Earth. The two main types of Chls, Chls *a* and *b*, with the molecular structures shown in Figure 1a,b, have been investigated under various studies using both steady-state[1−3] and time-resolved techniques.[4−6] The solvation relaxation timescales of Chls were reported to be in the range of several picoseconds. Recently, using advanced spectroscopic techniques,[7−14] the relaxation dynamics of Chls have been resolved in more details at various timescales spanning from sub-ps to tens of ps with several processes, including those involving hydrogen bonding and solvent polarity.[9,12] However, the assignments to specific molecular processes have remained elusive. Here, we perform 2DES measurements that study a specific molecular process, that of the fluctuation dynamics of a dative bond between the lone pair of a Lewis base and the Mg^{2+} center of a Chl molecule.

We investigate the ultrafast spectral diffusion dynamics of Chls *a* and *b* via center line slope (CLS) analysis[15] to track the time-dependent 2D peakshape evolution, which can provide detailed information about the solvation dynamics. Theoretical and experimental details can be found in the Supporting Information. A 2D spectrum, $S^{2D}(\omega_\tau, T_w, \omega_t)$, recorded at a series of waiting times T_w can be viewed as a frequency correlation map showing the probabilistic distribution of detection frequency ω_t after a delay T_w upon the initial excitation at ω_τ.

Figure 2 shows representative 2D spectra of Chl *a* in three different solvents, THF, 3F-Pyr, and Pyr, at T_w = 0.2, 10, and 60 ps, with the corresponding center lines overlaid. The CLS is proportional to the normalized frequency-fluctuation correlation function (FFCF), and the 2D peakshape at early T_w is diagonally elongated, yielding the higher slope of the center line. At later T_w, the 2D peakshape gradually becomes rounder due to the loss of correlation between the excitation and detection frequencies, and the CLS value tends toward zero, as shown in Figure 3. However, in the different solvents, the 2D peakshape evolves differently with delay time T_w, as shown in Figures 2 and 3. The time-evolution of the CLS value of every 2D measurement is fitted with a multiexponential decay function. We determine that a triexponential decay function is necessary to fit the CLS (in the Supporting Information, we provide justifications that a biexponential decay function fit is insufficient), $\mathrm{CLS}(T_w) = \sum_{i=1}^{3} A_i \exp(-T_w/\tau_i) + A_4$, and the obtained results are presented in Tables S2 and S3 for Chls *a* and *b*, respectively. Within the experimental time window,

Received: October 27, 2020
Accepted: December 3, 2020
Published: December 15, 2020

https://dx.doi.org/10.1021/acs.jpclett.0c03243
J. Phys. Chem. Lett. 2021, 12, 165−170

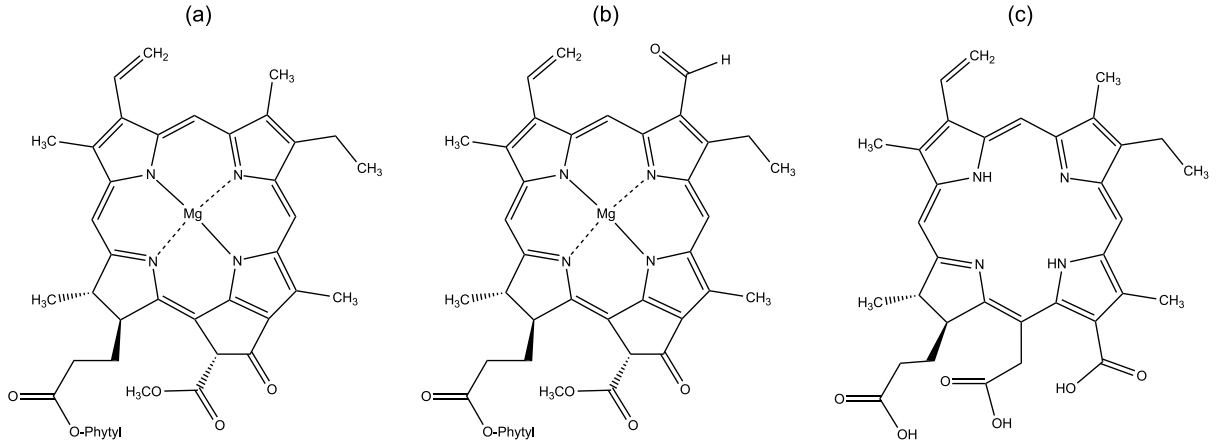

Figure 1. Molecular structures of the chromophores used in this study: Chl *a* (a), Chl *b* (b), and Chlorin-e6 (c).

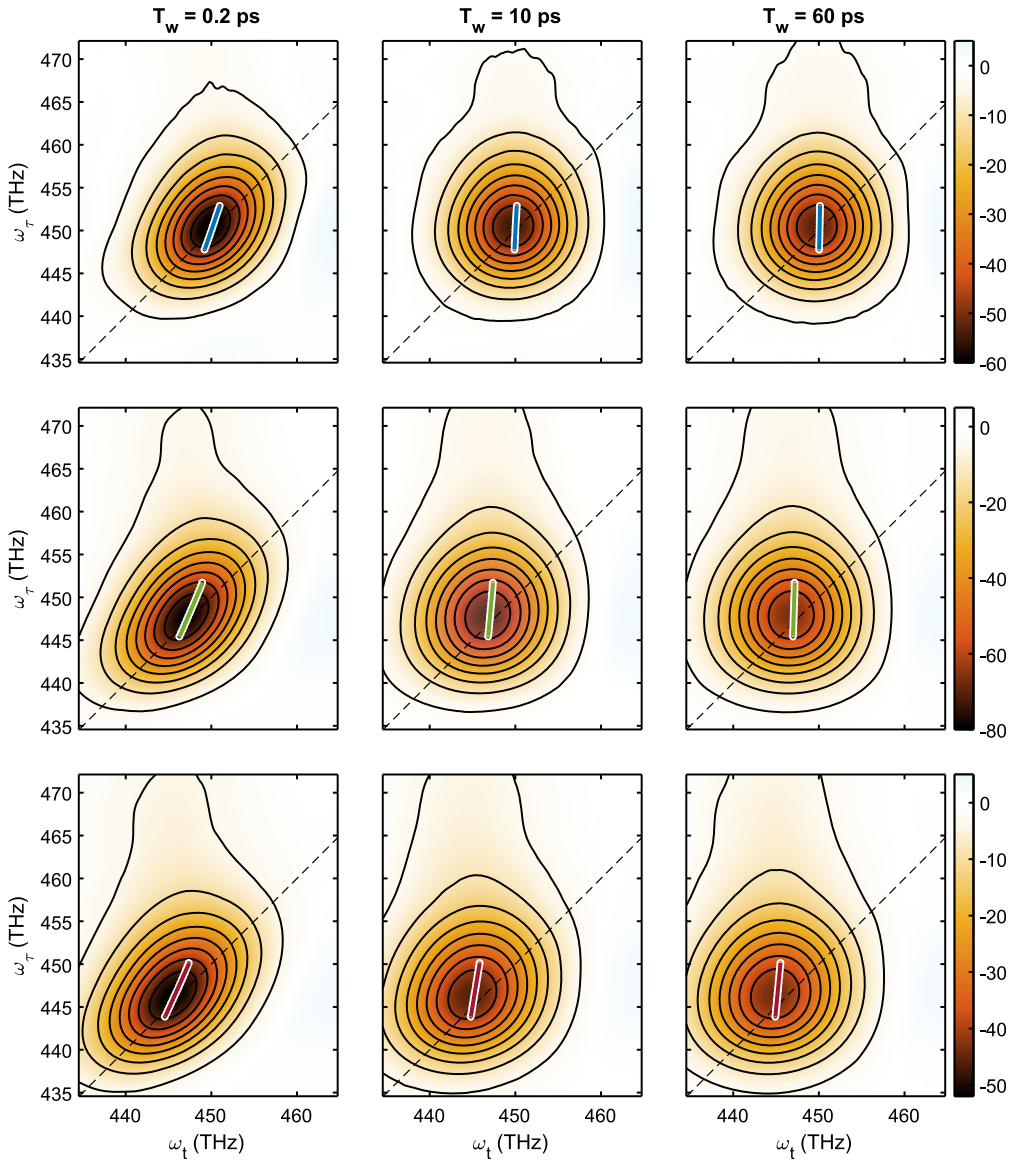

Figure 2. Representative 2D spectra of Chl *a* dissolved in tetrahydrofuran (THF) (first row), 3-fluoropyridine (3F-Pyr) (second row), and pyridine (Pyr) (third row) at T_w = 0.2, 10, and 60 ps. The white circles indicate the center points, ω_t^{max}, where the amplitudes of the horizontal slices peak (see Supporting Information). The straight lines are plotted in different colors for each solvent—THF (blue), 3F-Pyr (green), and Pyr (dark red)—representing the linear fit to obtain the CLS values at each T_w.

https://dx.doi.org/10.1021/acs.jpclett.0c03243
J. Phys. Chem. Lett. 2021, 12, 165−170

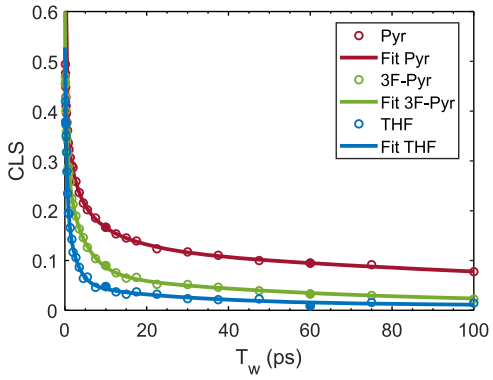

Figure 3. Center line slope (CLS) values vs T_w (circles) of Chl *a* dissolved in THF, 3F-Pyr, and Pyr, plotted with the same colors as in Figure 2, overlaid with the triexponential fits (lines). The filled circles denote the representative data of the 2D spectra plotted in Figure 2. Each of the CLS value data points is determined with an error of below 0.005.

apart from the three resolved exponential decay lifetimes, a baseline constant A_4 representing an inhomogeneous component is needed to complete the fit.

The first spectral diffusion lifetime τ_1 is resolved at the sub-ps timescale ranging between ~0.2 and 1.0 ps. This timescale has been commonly observed in three-pulse photon echo peak shift (3PEPS) experiments on various dyes[16] and attributed to inertial solvation dynamics.[17] The slowest timescale of nanoseconds is undetermined, as it is outside of our observed T_w range. This long-lived component is usually assigned as a measure of the structural inhomogeneity of the chromophore and usually relaxes at a nanosecond timescale.[10−12] The second and third diffusion lifetimes, τ_2 and τ_3, in the timescale of several to tens of ps are assigned to solvation relaxation processes. However, exact assignments to the molecular mechanisms of these processes remain elusive, and there are very limited evidential studies about the solvation mechanism at the molecular scale.[18,19]

The pK_a of the corresponding conjugate acid or BF_3 affinity is usually used to measure the Lewis basicity of an aprotic organic compound.[20] In Figure 4, the third spectral diffusion lifetimes, τ_3, of Chls *a* and *b* (and Chlorin-e6) are plotted against the solvents' Lewis basicity, measured through the pK_a of the conjugate acids and the BF_3 affinities. We notice, as a general trend in both Chls, that the third diffusion lifetime τ_3 increases with the solvents' Lewis basicity. This observable is of particular interest in this study, as further analysis and discussion can provide some insights about the relaxation mechanism at the molecular level.

As reported in previous studies,[3,13,21] when Chls are dissolved in nucleophilic solvents, the solvent molecules act as ligands, coordinating to the electrophilic Mg^{2+} center of the chlorin ring. In solvents having higher Lewis basicity (the group of pyridines), the heteroatom (nitrogen atom) of the ligand has a strong electron-donating ability and forms a stronger dative bond to the electrophilic Mg^{2+} center. On the other hand, in weaker Lewis bases (the group of ethers), the ligand−Mg^{2+} interaction is weaker due to the weaker electron-donating ability of the oxygen atom.

Together with the chemical considerations and the observations that the values of τ_3 trend with the solvents' Lewis basicity, we hypothesize that this spectral diffusion component, associated with the Lewis basicity trend, is due to the fluctuation of the dative bond connecting the heteroatom of the aprotic solvent molecule and the Mg^{2+} center of Chls. This fluctuation, involving bond lengthening, bond shortening, and angular changes, perturbs the electron density distribution of the chlorin macrocycle, which in turn affects the energies of the highest-occupied and the lowest-unoccupied molecular orbitals (MOs), which determine the absorption frequency of the Q_y transition in Chls.[22,23] The stronger dative bond between the Mg^{2+} center and solvent, i.e., higher Lewis basicity, leads to the slower fluctuation, resulting in a longer FFCF decay timescale τ_3, where the chromophore loses the "memory" of its initial excitation frequency more slowly.

To further support the hypothesis about the correlation between τ_3 and pK_a being caused by the Mg^{2+}−solvent dative bond fluctuation process, we carried out 2DES experiments on Chlorin-e6 as a control. Chlorin-e6 has a similar structure to Chl *a* (shown in Figure 1c) but without the Mg^{2+} cation in the center of the macrocycle.

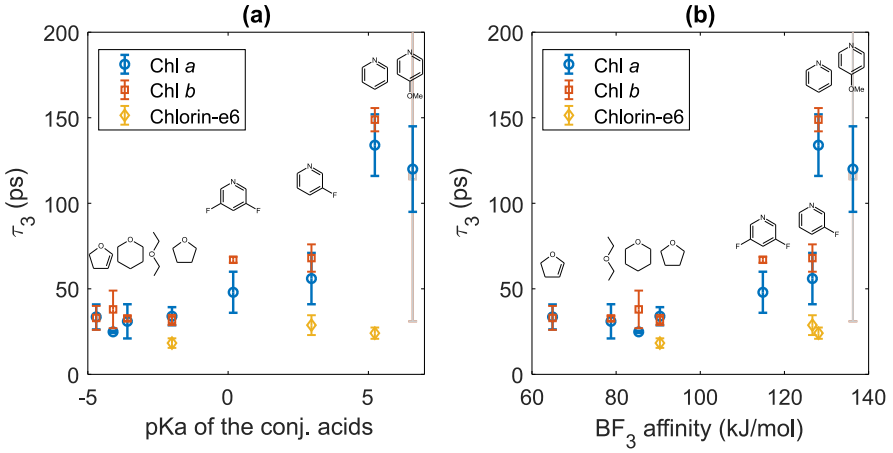

Figure 4. Trend between the third spectral diffusion lifetimes τ_3 of Chls *a* and *b* and the solvents' Lewis basicity reflected by (a) the pK_a of the solvents' conjugate acids and (b) the solvents' BF_3 affinities, contrasted with the solvent-independent diffusion lifetime of Chlorin-e6. The data point of Chl *b* in 4-methoxypyridine is plotted in gray due to the strongly distorted 2D peakshape, and the spectral diffusion lifetime cannot be determined with high accuracy (discussed in the Supporting Information).

https://dx.doi.org/10.1021/acs.jpclett.0c03243
J. Phys. Chem. Lett. 2021, 12, 165−170

2DES measurements were performed on Chlorin-e6 in THF, 3F-Pyr, and Pyr, and the third diffusion lifetimes τ_3 are directly compared with those for Chls *a* and *b* in Figure 4. In Figure 5, we depict the CLS curves of Chls *a* and *b* and Chlorin-e6 with the constant offsets A_4, accounting for static inhomogeneity, subtracted for a clearer comparison. For both Chls *a* and *b* (Figure 5a,b), there are clear differences in the curves for T_w > 20 ps, as the values of τ_3 strongly vary from ∼30 ps in THF to ∼150 ps in Pyr. In contrast, the CLS curves for Chlorin-e6 are essentially solvent independent, with the three curves in Figure 5c largely overlapping with each other despite the large changes in the solvents' Lewis basicity. (The data in Figure 5 is presented on a logarithmic scale as Figure S2 in the Supporting Information, for comparison.) The observation is attributed to the absence of the Mg^{2+} center in Chlorin-e6, which therefore does not experience coordination from the ligands to a Mg^{2+} center. This explains the relatively constant values of τ_3 even with strong variations in Lewis basicity of the solvents. The τ_3 process observed in Chlorin-e6 may be due to other intramolecular relaxation/reorganization dynamics. We should also point out that the τ_3 values for Chlorin-e6 are similar to those of Chls *a* and *b* in the ether solvents (see Figure 4). It is possible that these other interactions are also present in the case of Chls *a* and *b*. Although the strong Lewis basicity of the pyridine solvents masks these effects, the weak Lewis basicity of the ether solvents may allow these other interactions to be observed in Chls *a* and *b*. In general, solvation dynamics can have several processes happening simultaneously and spanning over a broad range of timescales.[24] The spectral diffusion timescale can also be affected by other physical properties of the solvent, such as viscosity, polarity, or hydrogen bonding.[9] However, in this study, all solvents are aprotic, together with the fact that the τ_3 values of Chlorin-e6 data are quite constant despite the strong variation of polarity and viscosity between THF and Pyr (see Table S1 of Supporting Information). This suggests that the effects of other solvents' physical properties are minor in the particular τ_3 diffusion timescale.

The observation discussed above supports our hypothesis that the third correlation lifetime τ_3 at the tens to hundreds of ps timescale is predominantly due to the dative bond fluctuation dynamics connecting the solvent molecule and the Chl Mg^{2+} center. Associated with τ_3 is the amplitude A_3 of the decay component, which is the normalized value of the energy fluctuation amplitude Δ_3 (eqs S1 and S2 of Supporting Information). Δ_3 in the FFCF (eq S1) gives a measure of how large a perturbation and fluctuation the associated process exerts on the electronic transition frequency, via how strong

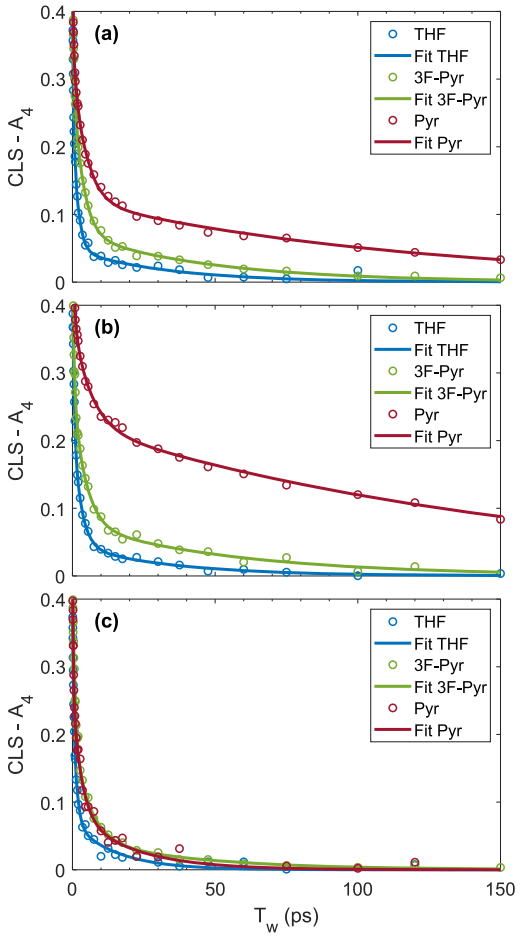

Figure 5. Comparison between the CLS analysis results of Chl *a* (a), Chl *b* (b), and Chlorin-e6 (c) in THF, 3F-Pyr, and Pyr (experimental values represented as circles overlaid with the triexponential fit lines). The Chls *a* and *b* results (a, b) show significant solvent dependence in dynamics, whereas the Chlorin-e6 results (c) are essentially solvent-independent.

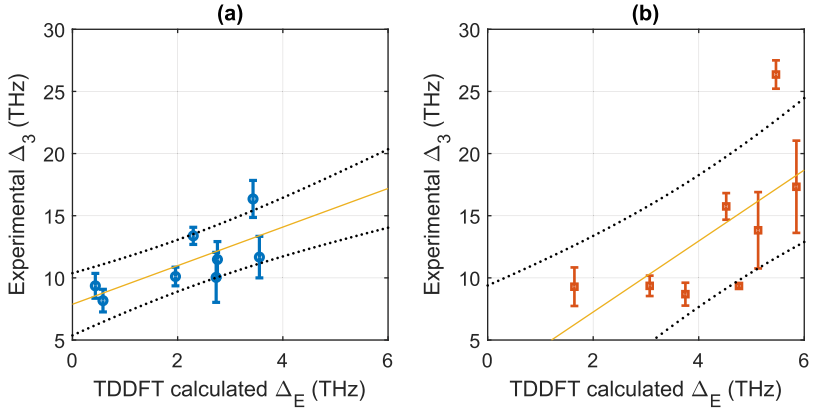

Figure 6. Comparison between the experimental fluctuation amplitude Δ_3 and the energy difference Δ_E between the penta- and hexacoordinated Chls obtained from TDDFT calculations for Chls *a* (a) and *b* (b). The linear fit (yellow line) shows the correlation between the experimental and TDDFT-calculated values with the 95% confidence interval (black dotted line).

https://dx.doi.org/10.1021/acs.jpclett.0c03243
J. Phys. Chem. Lett. 2021, 12, 165−170

(or weak) the ligands influence the electron density of the chlorin ring. In this case, it is therefore expected that the stronger the dative bond is, the larger Δ_3 will be. Δ_3 can then be viewed as the range of Q_y transition frequencies corresponding to the extents of the dative bond length and angle fluctuating from its weakest to strongest. One can also view this as a continuum range of transition frequency changes from an associated to a dissociated ligand state. When dissolved in aprotic nucleophilic solvents, Chls exist in mostly the penta- and hexacoordinated states (one and two solvent molecules, respectively, ligated with the Mg^{2+} center of Chls in the axial positions) depending on solvent and temperature.[3,13,21] We perform *ab initio* time-dependent density functional theory (TDDFT) calculations to obtain the energy difference Δ_E between the Q_y transitions of the penta- and hexacoordinated forms of Chls, i.e., $\Delta_E = |E_{penta} - E_{hexa}|$. Δ_E will be a gauge of the change in Q_y transition frequency of Chl undergoing the dissociation/association of one ligand, which we will then compare with the experimental obtained fluctuation amplitude Δ_3.

From the normalized FFCF obtained from the CLS analysis together with the linear absorption spectra, the stochastic fluctuation amplitude Δ_i can be recovered (details in the Supporting Information).[10,14] Figure 6 presents the scatter plot comparing the *ab initio* TDDFT calculation for energy difference Δ_E and experimental fluctuation amplitude Δ_3. In both panels of Figure 6, a linear fit (yellow line) shows the degree of correlation $R^2 = 0.50$ (Figure 6a) and $R^2 = 0.42$ (Figure 6b) for Chls *a* and *b*, respectively. This indicates that there is a qualitative correlation trend between the experimental fluctuation amplitudes Δ_3 and TDDFT-calculated Δ_E.

In Figure 6, the general trend of higher sensitivity of Chl *b* compared to Chl *a* is also correctly predicted by the *ab initio* TDDFT calculation, as well as observed in experimental results. The Chl *a* data points are mostly scattered between $\Delta_E = 0.5$ and 4 THz according to the TDDFT predictions and between $\Delta_3 = 7$ and 15 THz. Meanwhile, the Chl *b* results are spread between $\Delta_E = 2$ and 6 THz and $\Delta_3 = 10$ and 20 THz. This result agrees well with our observations that, due to the electron-withdrawing formyl group at the 7-carbon,[25] the Mg^{2+} center in Chl *b* is more deshielded, and the dative bond between the solvent molecule and Mg^{2+} center is stronger in Chl *b*. In addition, as depicted in Figure 6, the stronger dative bond in Chl *b* not only causes a slower spectral diffusion, i.e., larger τ_3, but also exhibits a stronger influence on the MO energy of the chlorin ring, causing the greater values of Δ_3.

For Chls *a* and *b* in the investigated solvents, the spectral diffusion processes taking place at the tens of ps timescale is attributed to the dynamic weakening and strengthening of the Mg^{2+}–ligand dative bond. The correlation of Δ_3 with the calculated Δ_E suggests that the dynamic weakening and strengthening of the Mg^{2+}–ligand dative bond can be viewed as the difference between dissociated and associated ligand states. The correlation timescale τ_3 is the characteristic time taken to sample over the fluctuation amplitude Δ_3 that spans the dissociated and associated ligand states and can be interpreted as the dynamic timescale of the breaking/forming of the Mg^{2+}–ligand dative bonds.

Comparing with a recent comprehensive study about the hydrogen bond network in H_2O, using 2D infrared (2D-IR) spectroscopy to probe the vibrational modes of anionic and neutral species, the spectral diffusion timescales in our study are in relatively good agreement.[26] Together with molecular dynamics simulation, three different spectral diffusion timescales of sub-ps, several ps, and tens of ps were determined. These three timescales were assigned to the different modulations induced by the hydrogen bond network in water. The slowest timescale, in the tens of ps range, is assigned to the vibration of the hydrogen bonds directly connecting the probe anions with the H_2O molecules in the first hydration shell. This is analogous to our τ_3 timescale describing the fluctuation of the dative bond connecting the solvent molecule and the Mg^{2+} center of the Chls. The lifetime of vibrational excitation in the 2D-IR study is typically less than 10 ps, leading to challenges in determining the last spectral diffusion lifetime due to low signal-to-noise ratios. In 2DES, the electronic excitation in Chl has lifetimes up to nanoseconds, thus providing an advantage in measuring the dynamics in the tens to hundreds of ps window. Hence, the 2DES method can be a good alternative to probe the slower dynamics, complementing the capability of 2D-IR spectroscopy.

The ascribed dynamics of the fluctuation of the dative bond connecting solvent molecule(s) and the Mg^{2+} center of Chls suggests a great potential of 2DES to provide valuable insights into specific molecular processes in various chemical and biological systems. For instance, the spectral diffusion lifetime can be used to estimate the ligation ability of not only common solvents but also synthetic ligands subjected to the dative bond lability. The chromophores are also not restricted to Chls *a* and *b*. Well-characterized molecules exhibiting a well-defined absorption band (Q_y transition in the case of Chls) which are sensitive to the ligation dynamics of the ligands can potentially be used.[27] In addition, probing ligation ability can provide insights about the local environment of the binding site within biological protein complexes,[28] which can be useful for docking and scanning of medicinal molecules.[29,30] However, 2DES-based spectral diffusion studies rely on the specific molecular processes under study to perturb the transition frequency sufficiently to be measured. To achieve this, development in increasing the signal-to-noise ratio of 2DES measurements and different combinations of analysis methods together with appropriately selected control experiments and calculations will be necessary.

■ ASSOCIATED CONTENT

Supporting Information

The Supporting Information is available free of charge at https://pubs.acs.org/doi/10.1021/acs.jpclett.0c03243.

Experimental details, theoretical information on spectral diffusion and CLS analysis results, justifications of triexponential fits, distortion of 2D peakshape due to ESA, reconstruction of energy fluctuation amplitudes, BF_3 affinity calculations, and *ab initio* TDDFT calculations (PDF)

■ AUTHOR INFORMATION

Corresponding Author

Howe-Siang Tan − *Division of Chemistry and Biological Chemistry, School of Physical and Mathematical Sciences, Nanyang Technological University, Singapore 637371;* orcid.org/0000-0003-2523-106X; Email: howesiang@ntu.edu.sg

https://dx.doi.org/10.1021/acs.jpclett.0c03243
J. Phys. Chem. Lett. 2021, 12, 165−170

Authors

Thanh Nhut Do − *Division of Chemistry and Biological Chemistry, School of Physical and Mathematical Sciences, Nanyang Technological University, Singapore 637371;* orcid.org/0000-0002-5155-6936

Jamie Hung Ni Sim − *Division of Chemistry and Biological Chemistry, School of Physical and Mathematical Sciences, Nanyang Technological University, Singapore 637371*

Hoang Long Nguyen − *Division of Chemistry and Biological Chemistry, School of Physical and Mathematical Sciences, Nanyang Technological University, Singapore 637371;* orcid.org/0000-0003-3635-6087

Yunpeng Lu − *Division of Chemistry and Biological Chemistry, School of Physical and Mathematical Sciences, Nanyang Technological University, Singapore 637371;* orcid.org/0000-0003-2493-7853

Complete contact information is available at: https://pubs.acs.org/10.1021/acs.jpclett.0c03243

Notes

The authors declare no competing financial interest.

■ ACKNOWLEDGMENTS

We acknowledge support from the Singapore Ministry of Education Academic Research Fund (Tier 1 RG2/19 and Tier 1 RG15/18).

■ REFERENCES

(1) Seely, G. R. Calculation of equilibrium constants for the solvation of chlorophyll from spectral data. *Spectrochim. Acta* **1965**, *21*, 1847−1856.

(2) Seely, G. R.; Jensen, R. G. Effect of solvent on the spectrum of chlorophyll. *Spectrochim. Acta* **1965**, *21*, 1835−1845.

(3) Renge, I.; Avarmaa, R. Specific Solvation of Chlorophyll a: Solvent Nucleophility, Hydrogen Bonding and Steric Effects on Absorption Spectra. *Photochem. Photobiol.* **1985**, *42*, 253−260.

(4) Oksanen, J. A. I.; Martinsson, P.; Åkesson, E.; Hynninen, P. H.; Sundström, V. Transient Hole Burning and Solvation Dynamics of Chlorophyll b Monomers in Various Solvent Environments. *J. Phys. Chem. A* **1998**, *102*, 4328−4336.

(5) Martinsson, P.; Oksanen, J. A. I.; Hilgendorff, M.; Hynninen, P. H.; Sundström, V.; Åkesson, E. Dynamics of ground and excited state chlorophylla molecules in pyridine solution probed by femtosecond transient absorption spectroscopy. *Chem. Phys. Lett.* **1999**, *309*, 386−394.

(6) Du, J.; Teramoto, T.; Nakata, K.; Tokunaga, E.; Kobayashi, T. Real-Time Vibrational Dynamics in Chlorophyll a Studied with a Few-Cycle Pulse Laser. *Biophys. J.* **2011**, *101*, 995−1003.

(7) Lazonder, K.; Pshenichnikov, M. S.; Wiersma, D. A. Easy interpretation of optical two-dimensional correlation spectra. *Opt. Lett.* **2006**, *31*, 3354.

(8) Loparo, J. J.; Roberts, S. T.; Tokmakoff, A. Multidimensional infrared spectroscopy of water. I. Vibrational dynamics in two-dimensional IR line shapes. *J. Chem. Phys.* **2006**, *125*, 194521.

(9) Moca, R.; Meech, S. R.; Heisler, I. A. Two-Dimensional Electronic Spectroscopy of Chlorophyll a: Solvent Dependent Spectral Evolution. *J. Phys. Chem. B* **2015**, *119*, 8623−8630.

(10) Nowakowski, P. J.; Khyasudeen, M. F.; Tan, H.-S. The effect of laser pulse bandwidth on the measurement of the frequency fluctuation correlation functions in 2D electronic spectroscopy. *Chem. Phys.* **2018**, *515*, 214−220.

(11) Do, T. N.; Khyasudeen, M. F.; Nowakowski, P. J.; Zhang, Z.; Tan, H. S. Measuring Ultrafast Spectral Diffusion and Correlation Dynamics by Two-Dimensional Electronic Spectroscopy. *Chem. - Asian J.* **2019**, *14*, 3992−4000.

(12) Khyasudeen, M. F.; Nowakowski, P. J.; Nguyen, H. L.; Sim, J. H. N.; Do, T. N.; Tan, H.-S. Studying the spectral diffusion dynamics of chlorophyll a and chlorophyll b using two-dimensional electronic spectroscopy. *Chem. Phys.* **2019**, *527*, 110480.

(13) Lewis, N. H. C.; Fleming, G. R. Two-Dimensional Electronic-Vibrational Spectroscopy of Chlorophyll a and b. *J. Phys. Chem. Lett.* **2016**, *7*, 831−837.

(14) Wells, K. L.; Zhang, Z.; Rouxel, J. R.; Tan, H.-S. Measuring the Spectral Diffusion of Chlorophyll a Using Two-Dimensional Electronic Spectroscopy. *J. Phys. Chem. B* **2013**, *117*, 2294−2299.

(15) Kwak, K.; Park, S.; Finkelstein, I. J.; Fayer, M. D. Frequency-frequency correlation functions and apodization in two-dimensional infrared vibrational echo spectroscopy: A new approach. *J. Chem. Phys.* **2007**, *127*, 124503.

(16) Nagasawa, Y.; Watanabe, A.; Takikawa, H.; Okada, T. Solute Dependence of Three Pulse Photon Echo Peak Shift Measurements in Methanol Solution. *J. Phys. Chem. A* **2003**, *107*, 632−641.

(17) Passino, S. A.; Nagasawa, Y.; Joo, T.; Fleming, G. R. Three-Pulse Echo Peak Shift Studies of Polar Solvation Dynamics. *J. Phys. Chem. A* **1997**, *101*, 725−731.

(18) Maroncelli, M.; Fleming, G. R. Picosecond solvation dynamics of coumarin 153: The importance of molecular aspects of solvation. *J. Chem. Phys.* **1987**, *86*, 6221−6239.

(19) Jimenez, R.; Fleming, G. R.; Kumar, P. V.; Maroncelli, M. Femtosecond solvation dynamics of water. *Nature* **1994**, *369*, 471−473.

(20) Laurence, C.; Gal, J. F. *Lewis Basicity and Affinity Scales: Data and Measurement*; Wiley, 2009.

(21) Saito, K.; Suzuki, T.; Ishikita, H. Absorption-energy calculations of chlorophyll a and b with an explicit solvent model. *J. Photochem. Photobiol., A* **2018**, *358*, 422−431.

(22) Blankenship, R. E. *Molecular Mechanisms of Photosynthesis*; Wiley, 2014.

(23) Kobayashi, M.; Akiyama, M.; Kano, H.; Kise, H. Spectroscopy and Structure Determination. In *Chlorophylls and Bacteriochlorophylls*; Grimm, B., Porra, R. J., Rüdiger, W., Scheer, H., Eds.; Springer: Dordrecht, 2006; Vol. *25*.

(24) Hoffman, D. J.; Fayer, M. D. CLS Next Gen: Accurate Frequency-Frequency Correlation Functions from Center Line Slope Analysis of 2D Correlation Spectra Using Artificial Neural Networks. *J. Phys. Chem. A* **2020**, *124*, 5979−5992.

(25) Nič, M.; Jirát, J.; Košata, B.; Jenkins, A.; McNaught, A., Eds. *IUPAC Compendium of Chemical Terminology (Gold Book, Advanced XML Version)*; International Union of Pure and Applied Chemistry, 2009.

(26) Okuda, M.; Higashi, M.; Ohta, K.; Saito, S.; Tominaga, K. Vibrational Frequency Fluctuations of Ionic and Non-ionic Vibrational Probe Molecules in Aqueous Solutions. *Coherent Multidimensional Spectroscopy*; Springer, 2019; Vol. *226*, pp 259−285.

(27) Reimers, J. R.; Cai, Z.-L.; Kobayashi, R.; Rätsep, M.; Freiberg, A.; Krausz, E. Assignment of the Q-Bands of the Chlorophylls: Coherence Loss via Q_x - Q_y Mixing. *Sci. Rep.* **2013**, *3*, 2761.

(28) Crouch, R. K.; Scott, R.; Ghent, S.; Govindjee, R.; Chang, C.-H.; Ebrey, T. Properties of Synthetic Bacteriorhodopsin Pigments. Further Probes of the Chromophore Binding Site. *Photochem. Photobiol.* **1986**, *43*, 297−303.

(29) Ruppert, J.; Welch, W.; Jain, A. N. Automatic identification and representation of protein binding sites for molecular docking. *Protein Sci.* **1997**, *6*, 524−533.

(30) Campbell, S. J.; Gold, N. D.; Jackson, R. M.; Westhead, D. R. Ligand binding: functional site location, similarity and docking. *Curr. Opin. Struct. Biol.* **2003**, *13*, 389−395.